

# Effect of B-site Dopants on Magnetic and Transport Properties of $\text{LaSrCoRuO}_6$

P S Ramu Murthy<sup>1</sup>, K R Priolkar<sup>1</sup>, P. A. Bhobe<sup>2</sup>, A. Das<sup>3</sup>, P. R. Sarode<sup>1</sup>, and A. K. Nigam<sup>2</sup>

<sup>1</sup> Department of Physics, Goa University, Taleigao Plateau, Goa 403 206, India

<sup>2</sup> Tata Institute of Fundamental Research, Homi Bhabha Road, Colaba, Mumbai 400 005 India

<sup>3</sup> Solid State Physics Division, Bhabha Atomic Research Centre, Trombay, Mumbai 400 085 India

November 12, 2010

**Abstract.** Effect of Co, Ru and Cu substitution at B and B' sites on the magnetic and transport properties of  $\text{LaSrCoRuO}_6$  have been investigated. All the doped compositions crystallize in the monoclinic structure in the space group  $P2_1/n$  indicating a double perovskite structure. While the magnetization and conductivity increase in Co and Ru doped compounds, antiferromagnetism is seen to strengthen in the Cu doped samples. These results are explained on the basis of a competition between linear Co-O-Ru-O-Co and perpendicular Co-O-O-Co antiferromagnetic interactions and due to formation of Ru-O-Ru ferromagnetic networks.

**PACS.** 75.50.Ee Antiferromagnetic Materials – 75.50.Pp Magnetic semiconductors – 72.80.Ga Transition metal compounds

## 1 Introduction

Perovskites containing 3d (B) and 4d or 5d (B') transition metal cations attract attention because of the strong competition between antiferromagnetic and ferromagnetic coupling and a complex interplay of spin charge and orbital degrees of freedom [1]. Some of these perovskites like  $\text{Sr}_2\text{FeMoO}_6$  and  $\text{Sr}_2\text{FeReO}_6$  display itinerant ferromagnetism and large low field magnetoresistance [2,3]. These properties can be effectively altered by substituting the B or B' site ions with other transition metal ions [4,5].

Ruthenium based double perovskites are interesting and have been studied extensively for their unusual magnetic and transport properties.  $\text{Ru(V)}$  containing perovskites exhibit many interesting properties like itinerant electron magnetism and co-existence of antiferromagnetic order and superconductivity [6,7,8,9,10]. Similarly  $\text{Ru(IV)}$  based double perovskites containing a transition metal ion on the B' site present a wide variety of ground states that depend on Ru 4d and O 2p covalent mixing and the itinerancy of  $\pi^*$  electrons [11].

$\text{LaSrCoRuO}_6$  is another double perovskite that provides a unique opportunity to examine the interplay of cationic order, charge balance and complex magnetic interactions between two transition metal ions [12,13]. Its crystal structure is composed of corner-shared  $\text{CoO}_6$  and  $\text{RuO}_6$  octahedra arranged in a pseudocubic array in the rocksalt arrangement. The degree of ordering is known

to affect the magnetic and transport properties due to changes in magnetic interactions and in cationic valence. Effects of anti-site disorder on the magnetic and transport properties due to La or Sr doping in  $\text{LaSrCoRuO}_6$  have been investigated [12,14,15].  $\text{LaSrCoRuO}_6$  compound is a semiconductor with ideal valence states HS  $\text{Co}^{2+}$  ( $3d^7$  high-spin configuration) and  $\text{Ru}^{5+}$  ( $4d^3$ ) [18]. The change of composition (La or Sr doping) introduces mobile electrons in La richer samples or holes in Sr richer samples. Magnetically these compounds are reported to be antiferromagnetic with two magnetic face centered cubic (fcc) sublattices consisting of Co and Ru. Both the sublattices order with type II antiferromagnetic structure which would mean that the spins in [111] planes in succession Co-Ru-Co-Ru alternate as  $+/+/-/-$ . This marginalizes the Co-O-Ru nearest neighbor interactions and the ordering is governed by a competition between linear Co-O-Ru-O-Co and  $90^\circ$  Co-O-O-Co antiferromagnetic exchange paths [12, 15].

Effect of substitutions at the B or B' sites in  $\text{LaSrCoRuO}_6$  have not been studied so far. In particular, the effect of antisite disorder will be very important as it will alter the magnetic interactions present in  $\text{LaSrCoRuO}_6$  and perhaps result in more complex magnetic ground state. Antisite disorder in ferromagnetic double perovskites like  $\text{Sr}_2\text{FeMoO}_6$  is known to affect magnetic and transport properties of these compounds [16]. Herein we report, structural, transport and magnetic properties of  $\text{LaSrCo}_{1-x}\text{Ru}_{1+x}$  for  $-0.3 \leq x \leq 0.4$  and  $\text{LaSrCo}_{1-y}\text{Cu}_y\text{RuO}_6$   $y \leq 0.2$  studied using X-ray diffraction (XRD), Neutron diffraction (ND), resistivity and magnetization as a function of

temperature and magnetic field. The compounds studied herein have a fixed A-site variance though varying Goldschmidt tolerance factor  $t$  [17] and redox active Co<sup>2+/3+</sup> and Ru<sup>4+/5+</sup> couples resulting essentially due to anti-site disorder. This study elucidates the complex role of coexisting localized electrons belonging to both Co and Ru  $d$  orbitals as well as some itinerant  $\pi^*$  electrons of Ru:t<sub>2g</sub> parentage that arise due to presence of Ru<sup>4+/5+</sup> and Co<sup>2+/3+</sup> redox couples on the structural, magnetic and transport properties of substituted LaSrCoRuO<sub>6</sub>.

## 2 Experimental

Polycrystalline samples of LaSrCo<sub>1-x</sub>Ru<sub>1+x</sub>O<sub>6</sub>;  $-0.3 \leq x \leq 0.4$  and LaSrCo<sub>1-y</sub>Cu<sub>y</sub>RuO<sub>6</sub>;  $y = 0.1$  and  $0.2$  were synthesized by firing well mixed stoichiometric amounts of La<sub>2</sub>O<sub>3</sub>, SrCO<sub>3</sub>, Co(NO<sub>3</sub>)<sub>3</sub>·6H<sub>2</sub>O, RuO<sub>2</sub> and CuO. These fired mixtures were then thoroughly ground and fired 1300°C followed by slow cooling to room temperature. The process grinding and firing was repeated three times. Prior to firing, the powders of La<sub>2</sub>O<sub>3</sub>, RuO<sub>2</sub> and SrCO<sub>3</sub> were pre-heated at 900°C and 700°C respectively to get rid of any adsorbed water. The samples were characterized by XRD for their structure and phase purity. The diffracted intensities were measured in the  $2\theta$  range of 15° to 80° using Cu K $\alpha$  radiation. The diffraction patterns were Rietveld refined using FULLPROF suite to obtain lattice parameters. ND measurements on some of the samples were carried out on the Powder diffractometer at Dhruva Reactor, Trombay using neutrons of wavelength 1.24Å in the temperature range 20K to 300K. DC magnetization was measured, both, as a function of temperature and magnetic field using the Quantum Design SQUID magnetometer (MPMS-5S). M(T) was measured in an applied field of 50 Oe and 1000 Oe in the temperature range of 5 to 300 K. The sample was initially cooled from 300K to 5 K in zero applied field and the data was recorded while warming up to 300 K in the applied magnetic field (referred to as ZFC curve) and subsequent cooling (referred to as FC curve) back to 5 K. Magnetization as a function of field was measured under sweep magnetic fields up to  $\pm 5T$  at various temperatures. Before each M(H) was recorded, the sample was warmed to 300 K and cooled back to the desired temperature. The temperature dependence of the electrical resistivity in the range 10K - 300K was measured using a standard four probe set up.

## 3 Results

### 3.1 LaSrCo<sub>1-x</sub>Ru<sub>1+x</sub>O<sub>6</sub>

The stability of the ordered double perovskite phase with P2<sub>1</sub>/n symmetry is determined within the composition region  $x = 0.1$  to  $0.4$  for Ru and  $x = -0.1$  to  $-0.3$  for Co from the Le Bail refinement of XRD patterns which are presented in Fig. 1. The lattice parameters obtained from refinement are presented in Table 1. LaSrCoRuO<sub>6</sub> which

has Co<sup>2+</sup> and Ru<sup>5+</sup> ions occupying the B-site represents a perfectly ordered perovskite with NaCl type ordering of its B-sites cations. Substitution of Ru for Co and Co for Ru creates not only an antisite disorder in the Co-O-Ru matrix but also changes the formal valence of the B-site ions. While the effect of disorder can be clearly seen in Fig. 2 on the superlattice reflection ( $\frac{1}{2}, \frac{1}{2}, \frac{1}{2}$ ) at  $\sim 19.5^\circ$  and the Co and Ru occupancies at ( $\frac{1}{2}, 0, 0$ ) and ( $\frac{1}{2}, 0, \frac{1}{2}$ ) sites in Table 1, the linear variation of the cell volume with  $x$  as seen in Fig. 3(a) indicates a change in the formal valence of B-site cations. It may be noted here that Co<sup>3+</sup> has a smaller ionic radius than Co<sup>2+</sup> while the ionic radius of Ru<sup>4+</sup> is larger than Ru<sup>5+</sup> and hence the cell volume decreases for Co doped compounds and increases with Ru doping. The linear variation of the unit cell volume also confirms the existence of single-phase solid solutions for all values of composition  $x$  reported here. An interesting aspect of substitution of Co at the Ru site is the comparatively large change in the monoclinic cell angle,  $\beta$ . It decreases from 90.05° in the undoped sample to 89.9° for the Co doped sample ( $x = -0.2$ ) whereas remains nearly constant for the Ru doped samples. This could be due to the large charge and size difference between Co and Ru and/or due to a deviation from pseudo-cubic symmetry arising because of clustering of similar B-site ions due to charge balance. With increasing Co substitution from  $x = -0.1$  to  $-0.3$ , the electrons are likely to be removed from the Co ions leading to a valency increase of Co from 2+ to 3+ as the Ru ions are in highly oxidized state. But this does not satisfy the charge balance and will require some of the Ru<sup>5+</sup> to reduce to Ru<sup>4+</sup>. Consequently, the charge and the size difference between Ru and Co ion may lead to a deviation in  $\beta$ . This can be also be visualized in Fig. 3(b) where  $t$  is plotted as a function of composition  $x$ . While  $t$  increases from about 0.91 for  $x = 0$  to 0.95 for  $x = 0.4$  (Ru-rich compositions), it decreases to 0.89 for  $x = -0.3$  (Co-rich compositions) indicating that the substitution of Ru for Co allows for a better matching of A-O and B(B')-O bond distances than the replacement of Ru by Co.

The structural changes occurring due to Ru and Co doping will have an effect on the magnetic properties. Fig.4 presents the temperature variation of magnetization measured between 5K and 300K in an applied field of 1000Oe and the magnetic susceptibility ( $\chi = M/H$ ) calculated from thereon for four representative compounds. The difference between ZFC and FC magnetization curve reveals a complex magnetic structure. In the high temperature region ( $200K \leq T \leq 300K$ ),  $\chi$  was fitted to the Curie-Weiss equation

$$\chi = C/(T - \Theta_{CW})$$

where  $C = N_A(\mu_{eff}\mu_B)^2/3k_B$  is the Curie constant and  $\Theta_{CW}$  is the Curie-Weiss temperature. Effective moment per formula unit ( $\mu_{eff} = g[S(S+1)]^{1/2}$ ) calculated from  $C$  and  $\Theta_{CW}$  obtained for fitting for all the compounds along with undoped compound, LaSrCoRuO<sub>6</sub> and are enlisted in Table 1. From the analysis of the high temperature magnetization in the doped systems, it can be inferred that Co

**Table 1.** Room temperature structural parameters obtained from Le Bail fitting and high temperature magnetic and transport properties for LaSrCo<sub>1-x</sub>Ru<sub>1+x</sub>O<sub>6</sub>. Here  $a$ ,  $b$ ,  $c$  and  $\beta$  denote unit cell parameters,  $N_{\text{Ru}(\frac{1}{2},0,0)}$  denotes the occupancy of Ru at  $(\frac{1}{2},0,0)$  site,  $\mu_{eff}$  and  $\Theta_{CW}$  represent effective magnetic moment and Curie Weiss temperature respectively and  $T_p$  is temperature of peak magnetization seen in ZFC curve. Numbers in parentheses are uncertainty in the last digit.

$x$	-0.3	-0.2	-0.1	0	0.1	0.2	0.3	0.4
$a$ (Å)	5.5866(4)	5.5861(3)	5.5858(3)	5.5847(4)	5.5847(4)	5.5846(3)	5.5843(4)	5.584(3)
$b$ (Å)	5.5551(6)	5.5553(5)	5.5555(5)	5.5592(6)	5.5541(5)	5.5533(6)	5.5524(4)	5.5515(5)
$c$ (Å)	7.8599(5)	7.8612(5)	7.8634(5)	7.8673(4)	7.8646(4)	7.8641(5)	7.8629(5)	7.8636(4)
$\beta$	89.92(2)	89.98(1)	89.96(2)	90.05(2)	90.04(2)	90.04(1)	90.04(1)	90.05(1)
Volume (Å <sup>3</sup> )	243.68(4)	243.87(3)	244.12(3)	244.25(4)	244.31 (3)	244.43(3)	244.57(4)	244.74(3)
$N_{\text{Ru}(\frac{1}{2},0,0)}$	0.55	0.67	0.83	0.98	0.81	0.70	0.80	0.86
$N_{\text{Co}(\frac{1}{2},0,0)}$	0.45	0.33	0.17	0.02	0.19	0.30	0.20	0.14
$N_{\text{Co}(\frac{1}{2},0,\frac{1}{2})}$	0.85	0.87	0.93	0.98	0.71	0.70	0.50	0.46
$N_{\text{Ru}(\frac{1}{2},0,\frac{1}{2})}$	0.15	0.13	0.07	0.02	0.29	0.30	0.50	0.54
$\mu_{eff}$ ( $\mu_B/\text{fu}$ )	5.52(2)	5.35(1)	–	5.47(2)	5.50(2)	5.42(2)	5.39(2)	5.58(3)
$\Theta_{CW}$ (K)	24(1)	37(1)	–	-49(1)	21(1)	25(1)	25(1)	0(1)
$T_p$ (K)	42(1)	47(1)	–	70(1)	53(1)	52(1)	54(1)	49(1)

ions are in high spin (HS) or intermediate spin (IS) state and that the magnetic interaction for all  $x$  are dominated by nearest neighbor interactions of the superexchange type between HS/IS Co<sup>2+,3+</sup> and low spin (LS) Ru<sup>4+,5+</sup> ions. A second observation is that the effective magnetic moment does not vary with  $x$ . The nearly constant value of  $\mu_{eff}$  for  $x \in (-0.3 \text{ to } 0.4)$  region can only be explained on the basis of presence of HS and IS states for Co<sup>3+</sup> and Ru<sup>4+</sup>. In the case of undoped sample, the type of long range magnetic order is characterized by  $\Theta_{CW} \sim -50\text{K}$  and a clear antiferromagnetic transition at  $T_N \approx 80\text{K}$  [12]. In case of Ru and Co doped samples,  $\Theta_{CW}$  is positive indicating presence of additional ferromagnetic interactions. In Ru doped samples, positive  $\Theta_{CW}$  can be understood to be due to ferromagnetic Ru<sup>4+</sup>-O-Ru<sup>4+</sup> interactions. The presence of such interactions is supported by the sudden rise of magnetization at about 160K which is close to ferromagnetic ordering temperature of SrRuO<sub>3</sub>. The presence of any SrRuO<sub>3</sub> impurity phase however, can be ruled out as no additional reflections are seen in the diffraction pattern even at 40% Ru doping. The competition between the ferromagnetic and antiferromagnetic interactions can result in magnetic frustration below the peak temperature  $T_p \sim 50\text{K}$  seen in ZFC magnetization curve. The nature of magnetic order will be confirmed later using neutron diffraction. Positive values of  $\Theta_{CW}$  even in Co doped compounds is puzzling. It can only be understood to be due to presence of Co<sup>2+/3+</sup> and Ru<sup>4+/5+</sup> redox pairs for charge balance. The nearly constant values of  $\mu_{eff}$  supports this conjuncture well. Sudden rise seen in magnetization at around 160K seen in 20% and 30% Co doped samples is also in agreement with the above view. The presence of Ru<sup>4+</sup> leads to the ferromagnetic Ru-Ru interaction where the Ru 4d electrons form itinerant-electron  $\pi^*$  bands of t-orbital parentage. Presence of competition between ferromagnetic and antiferromagnetic interactions is also evident from magnetization curves of Co doped samples. Furthermore, the hysteresis loop recorded for 20% Co doped compound at 5K in magnetic field interval of  $\pm 5$  Tesla and

presented in Fig. 5 exhibits a small irreversibility (see the expanded loop in the inset of Fig. 5) indicating existence of weak ferromagnetic interactions along with antiferromagnetic interaction. In the case of Ru doped compound however, presence of clear magnetic hysteresis riding on smoothly increasing background indicates a strong competition between ferro and antiferromagnetic interactions.

In order to understand this competition further, magnetization was recorded in a low field of 50Oe. Here the magnetization response in the Ru doped samples is completely different as compared to that measured at 1000 Oe as can be seen in the Fig 6. During the ZFC cycle, the magnetization is negative at the lowest temperature and increases continuously with increase in temperature. At about 158K and crosses over to the positive side, exhibits a peak at 162K signifying a transition from a magnetically ordered to a paramagnetic state. The magnetization remains positive during the entire FC cycle exhibiting a relatively sharp rise at 162K, precisely the same temperature at which ZFC shows a cusp. In the case of Co doped samples, although there is a large difference between ZFC and FC magnetization curves, the magnetization is positive during both cycles. It may be emphasized here that care has been taken to make sure that the remanent field of SQUID magnetometer was less than  $\pm 13$  Oe during these low field measurements. Furthermore, in the inset of M versus T plot for  $x = 0.2$  shows the initial magnetization curve for the same sample measured as a function of field. It can be clearly seen that magnetization is negative in fields up to about 700 Oe.

Neutron diffraction was employed to determine the magnetic structure of two compounds,  $x = 0.2$  and  $-0.2$ . The data taken at 300K and 20K is presented in Fig. 7. The data at 20K is shown in very limited range in order to highlight the magnetic reflections. Very weak reflections due to AFM ordering were observed (marked in Fig. 7) in the positions given by the propagation vector along the pseudocubic 111 direction with respect to the crystallographic  $P2_1/n$  cell [12,19]. The observation of the lines

with  $k = (1/2, 0, 1/2)$  defines that AFM arrangement in each sublattice is of type II, consisting of ferromagnetic [111] planes. The values of magnetic moments at 20K obtained from neutron diffraction are  $\mu(\text{Co}) \sim \mu(\text{Ru}) = 1.0\mu_B$  for  $x = 0.2$  and  $\mu(\text{Co}) \sim \mu(\text{Ru}) = 0.6\mu_B$  for  $x = -0.2$ . This implies that the spins in (111) planes alternate as  $+/-/-/+$  for Co/Ru/Co/Ru. Such a AFM arrangement also indicates that the magnetic ordering is governed by the  $180^\circ$  Co-O-Ru-O-Co AFM exchange paths [20,21]. Earlier studies report the presence of competing  $90^\circ$  Co-O-O-Co AFM exchange paths that can be a cause of magnetic frustration leading to the low values of long-range-ordered moments as detected by neutron scattering [15].

The temperature dependence of the resistivity for LaSrCo<sub>1-x</sub>Ru<sub>1+x</sub>O<sub>6</sub> with  $x = -0.2, 0$  and  $0.2$  are plotted in the Fig 8. The samples exhibit semiconducting behavior in the entire measured range of temperature. The addition of Ru and Co dopants is found to decrease the resistivity significantly by about two orders of magnitude. In the case of Ru doped samples the decrease in resistivity is due to the formation of metallic Ru<sup>4+</sup> - O - Ru<sup>4+</sup> chains in these samples which essentially result due to excess Ru concentration. On the other hand in the case of Co doped samples, structural and magnetization studies indicated the presence of Co<sup>2+/3+</sup> and Ru<sup>4+/5+</sup> redox pairs. The presence of Ru<sup>4+</sup> results in itinerant electrons due to population of  $\pi^*$  antibonding orbitals. This explains the decrease in resistivity in case of Co doped samples.

### 3.2 LaSrCo<sub>1-y</sub>Cu<sub>y</sub>RuO<sub>6</sub>

In Fig. 9 XRD patterns of 10% and 20% Cu doped LaSrCoRuO<sub>6</sub> compounds is presented. Both these compounds are single phase and the structural parameters obtained from Le Bail fitting are presented in Table 2 along with that of undoped sample, LaSrCoRuO<sub>6</sub> for ready comparison. The unit cell volume in Cu doped samples is slightly lower. This could be because of slightly smaller ionic radii of Cu<sup>2+</sup> (0.73Å) than that of Co<sup>2+</sup> (0.745Å) in HS configuration. Substitution of Cu for Co is expected not to alter charge balance and therefore Ru will be in 5+ state as in undoped compound. However, the substitution is expected to alter magnetic and transport properties. Substitution of Cu in Sr<sub>2</sub>HoRuO<sub>6</sub> type double perovskites is reported to exhibit a coexistence of antiferromagnetism and superconductivity [10].

Magnetization for the two Cu doped samples, recorded during ZFC and FC cycles in an applied field of 1000 Oe is presented in Fig. 10. In both cases both ZFC and FC magnetization curves increases with decreasing temperature culminating into a broad peak centred at 42K and 47K respectively for  $y = 0.1$  and  $0.2$  samples. Inverse magnetization plotted for both the samples in lower panel of Fig. 10 shows linear variation down to 100K. The calculated susceptibility ( $\chi = M/H$ ) was fitted to Curie-Weiss equation. The values of  $\mu_{eff}$  and  $\Theta_{CW}$  extracted from fitting are listed in Table 2. The values of  $\Theta_{CW}$  obtained are both negative although much smaller than that of the undoped sample. Negative values indicate dominance of

**Table 2.** Room temperature structural parameters obtained from Le Bail fitting and high temperature magnetic and transport properties for LaSrCo<sub>1-x</sub>Ru<sub>1+x</sub>O<sub>6</sub>. Here  $a$ ,  $b$ ,  $c$  and  $\beta$  denote unit cell parameters,  $\mu_{eff}$  and  $\Theta_{CW}$  represent effective magnetic moment and Curie Weiss temperature respectively and  $T_p$  is temperature of peak magnetization seen in ZFC curve. Numbers in parentheses are uncertainty in the last digit.

$x$	0	0.1	0.2
$a$ (Å)	5.5847(4)	5.5621(2)	5.5627(2)
$b$ (Å)	5.5592(6)	5.5518(2)	5.5544(2)
$c$ (Å)	7.8673(4)	7.8684(2)	7.8714(2)
$\beta$	90.05(2)	90.23(1)	90.28(1)
Volume (Å <sup>3</sup> )	244.25(4)	242.98(4)	243.20(3)
$\mu_{eff}$ ( $\mu_B/\text{fu}$ )	5.47(2)	5.18(1)	5.01(1)
$\Theta_{CW}$ (K)	-49(1)	-32.1(3)	-7.3(4)
$T_p$ (K)	70(1)	47(1)	42(1)

antiferromagnetic interactions in these compounds. Theoretically calculated spin only moments using Ru<sup>5+</sup> ( $S = 3/2$ ), Co<sup>2+</sup> ( $S = 3/2$ ) and Cu<sup>2+</sup> ( $S = 1/2$ ) for both the doped samples are in good agreement with the experimentally obtained values. This behavior is unlike that seen in case of Ru and Cu doped compounds. The large splitting observed between ZFC and FC magnetization curves is absent. Dominant interaction is antiferromagnetic. Even with presence of a impurity ion (Cu<sup>2+</sup>) there appears to be no clustering or change in valence of Ru or Co.

In order to see the effect of Cu doping on the transport properties of LaSrCoRuO<sub>6</sub>, electrical resistivity in the temperature range 10K < T < 300K has been measured and presented in Fig. 11. It appears that with Cu substitution, there is very little change in resistivity as compared to the undoped sample. This can be attributed to Cu<sup>2+</sup> replacing Co<sup>2+</sup> ions inhibiting the conversion of Ru<sup>5+</sup> to Ru<sup>4+</sup> or formation of Ru-O-Ru chains.

## 4 Discussion

Substitution at B-site in ordered LaSrCoRuO<sub>6</sub> double perovskite allows an opportunity to probe the changes in structural, magnetic and transport properties due to creation of Co<sup>2+/3+</sup> and Ru<sup>4+/5+</sup> redox couples in an environment with fixed A-site variance and linearly varying Goldschmidt tolerance factor. In the entire doping region, for both the series, the double perovskite structure is preserved.

The magnetic and transport properties of LaSrCo<sub>1-x</sub>Ru<sub>1+x</sub>O<sub>6</sub> on the other hand show significant changes due to the creation of Ru<sup>4+</sup> and Co<sup>3+</sup> species in both Co doped and Ru doped compounds. The antisite disorder resulting due to excess Ru or Co leads to creation of Ru<sup>4+</sup> and Co<sup>3+</sup> species in addition to Ru<sup>5+</sup> and Co<sup>2+</sup> ions in order to maintain charge balance. In the case of undoped compound, LaSrCoRuO<sub>6</sub> there are two competing magnetic interactions, the linear Co-O-Ru-O-Co and the  $90^\circ$  Co-O-O-Co. In the

Ru and Co doped compounds these interactions get diluted at the expense of new interactions of the type  $\text{Ru}^{4+/5+}\text{-O-Ru}^{4+/5+}$  and those involving HS/IS  $\text{Co}^{3+}$ . The sharp rise in magnetization seen at about 160K in all Co and Ru doped compounds can be attributed to ferromagnetic interactions arising due to Ru-O-Ru nearest neighbor interactions. As in case of  $\text{SrRuO}_3$  such an interaction leads to filling up of  $\pi^*$  band and lowering of resistivity as compared to undoped  $\text{LaSrCoRuO}_6$ . The negative magnetization displayed by Ru rich compounds in low applied fields can then be understood to be due to polarization of paramagnetic Co spins by Ru-O-Ru ferromagnetic interactions below the Ru sublattice ordering temperature (160K). The Co spins are polarized in a direction opposite to applied magnetic field giving rise to magnetic compensation and negative magnetization. In the case of Co doped compounds, no negative magnetization is observed although there is the steep rise of magnetization below 160K. Instead, only a large variation between ZFC and FC magnetization curves is seen. This could be understood to be due to clustering of similar types of ions in the sample. This is also indicated by decrease in the strength of ferromagnetic interactions with increasing Co content.

The competition between magnetic interactions observed in case of Co and Ru substituted compounds is reduced or eliminated with Cu substituting Co in  $\text{LaSrCoRuO}_6$ . The magnetic properties clearly indicated presence of antiferromagnetic interactions from negative  $\Theta_{CW}$  and the magnetization behavior in the entire temperature range. Since  $\text{Cu}^{2+}$  substitutes  $\text{Co}^{2+}$ , the charge on Ru remains unaltered. Since the ionic sizes of the two ions are also similar, there are no major structural changes. This results in nearly similar magnitude of resistivity as in the case of undoped  $\text{LaSrCoRuO}_6$ .

It is known that partially filled 3d levels of Co in  $\text{SrRuO}_3$  are well below the conduction band of  $\text{Ru}^{4+}$ . Therefore it is favorable to transfer an electron from Ru to Co, even though such electrons may become localized. The resulting  $\text{Co}^{2+}$  state will move its level closer to but still below Ru 4d levels. Thus the presence of highly acidic  $\text{Ru}^{5+}$  is more stabilizing for high spin  $\text{Co}^{2+}$  leading to an ordered lattice. Doping of Co and Ru will result in formation of Co-O-Co and Ru-O-Ru networks respectively. From XANES studies reported in [13] it is clear that Co-Co pairs will favor the trivalent state, and likewise Ru-Ru pairs would favor the tetravalent states. Therefore the observed magnetic behavior reflects the general competition between the itinerant ferromagnetism and the antiferromagnetic superexchange coupling between Co-Co pairs, further modified by the interactions of between Ru and Co. Since Cu substitution does not favor formation of Ru-O-Ru or Co-O-Co networks but instead disturbs the existing magnetic interactions especially the  $90^\circ$  Co-O-O-Co interaction, antiferromagnetism appears to be strengthened.

## 5 Conclusion

The study of magnetic and transport properties of ceramic samples  $\text{LaSrCo}_{1-x}\text{Ru}_{1+x}\text{O}_6$  and  $\text{LaSrCo}_{1-y}\text{Cu}_y\text{RuO}_6$  leads to the following conclusions:

1. The ordered double perovskite phase exists for  $-0.3 \leq x \leq 0.4$ .
2. The thermally activated electrical resistivity is associated with nearest neighbor hopping between Co and Ru ions via linking oxygen atoms. The decrease in resistivity with Ru and Co doping is due to formation of  $\text{Ru}^{4+}$  and more holes in the Ru *d* band.
3. The Co and Ru doped compounds also show an increase in magnetization due to the formation of ferromagnetic Ru-O-Ru interactions.
4. In case of Cu doped compounds, the antiferromagnetism strengthens due to the suppression of the competing  $90^\circ$  Co-O-O-Co antiferromagnetic interactions.

PSRM and KRP acknowledge support from UGC-DAE Consortium for Scientific Research, Mumbai Centre for financial support under CRS-M-126. KRP and PRS would also like to thank Department of Science and Technology (DST), Government of India for financial support under the project No. SR/S2/CMP-42.

## References

1. D. D. Sarma, Curr. Opin. Solid State Mater. Sci **5** (2001) 261
2. K. L. Kobayashi, T. Kimura, H. Sawada, K. Terakura, Y. Tokura Nature **395** (1998) 677
3. J. Gopalakrishnan, A. Chattopadhyay, S. B. Ogale, T. Venkatesan, R. L. Greene, A. J. Millis, K. Ramesha, B. Hannoyer and G. Marest, Phys. Rev. B **62** (2000) 9538
4. F. Sriti, A. Maignan, C. Martin and B. Raveau, Chem. Mater. **13** (2001) 1746
5. X. M. Feng, G. H. Rao, G. Y. Liu, H. F. Yang, W. F. Liu, Z. W. Ouyang, L. T. Yang, Z. X. Liu, R. C. Yu, C. Q. Jin and J. K. Liang, J. Phys. Condens. Matter **14** (2002) 12503
6. P. D. Battle and W. J. Macklin, J. Solid State Chem. **52** (1984) 138
7. N. Kamagashira, T. Mori, A. Imamura, and Y. Hinatsu, J. Alloys Compd. **302**, (2002) L6
8. Y. Doi, Y. Hinatsu, K. Oikawa, Y. Shimojo and Y. Morii, J. Mater. Chem. **10** (2000) 797
9. M. K. Wu, D. Y. Chen, F. Z. Chien, S. R. Sheen, D. C. Ling, C. Y. Tai, G. Y. Tseng, D. H. Chen and F. C. Zhang, Z. Phys. B: Condens. Matter **102** (1997) 37
10. N. G. Parkinson, P. D. Hatton, J. A. K. Howard, C. Ritter, F. Z. Chien and M. K. Wu, J. Mater. Chem. **13** (2003) 1468
11. R. I. Dass, J. Q. Yan and J. B. Goodenough, Phys. Rev. B **69** (2004) 094416
12. J-W. G. Bos and J. P. Attfield, Chem. Matter. **16** (2004) 1822
13. A. Mamchik, W. Dmowski, T. Egami and I-W Chen, Phys. Rev. B **70** (2004) 104410

14. P. Tomeš, J. Hejtmánek and K. Knížek, Solid State Sci. **10** (2008) 486
15. M. Dlouhá, J. Hejtmánek, Z. Jiráček, K. Knížek, P. Tomeš and S. Vratilav S J. Magn. Mater. (2009) doi:10.1016/j.jmmm.2009.06.035
16. D. Serrate, J. M. de Teresa and M. R. Ibarra, J. Phys. Condens. Matter **19** (2007) 023201
17. V. M. Goldschmidt, Skrifter Nordske Videnskaps-Akad. Oslo I, Mat-Naturvidensk Kl., **8** (1926) 2
18. S. H. Kim and P. D. Battle, J. Sol. State. Chem **114** (1995) 174
19. J-W. G. Bos and J. P. Attfield, J. Mater. Chem. **15** (2005) 715
20. J-W. G. Bos, and J. P. Attfield, Phys. Rev. B **70** (2004) 174434
21. E. Rodriguez, M. L. Lopez, J. Campo, M. L. Veiga and C. Pico, J. Mater. Chem. **12** (2002) 2798

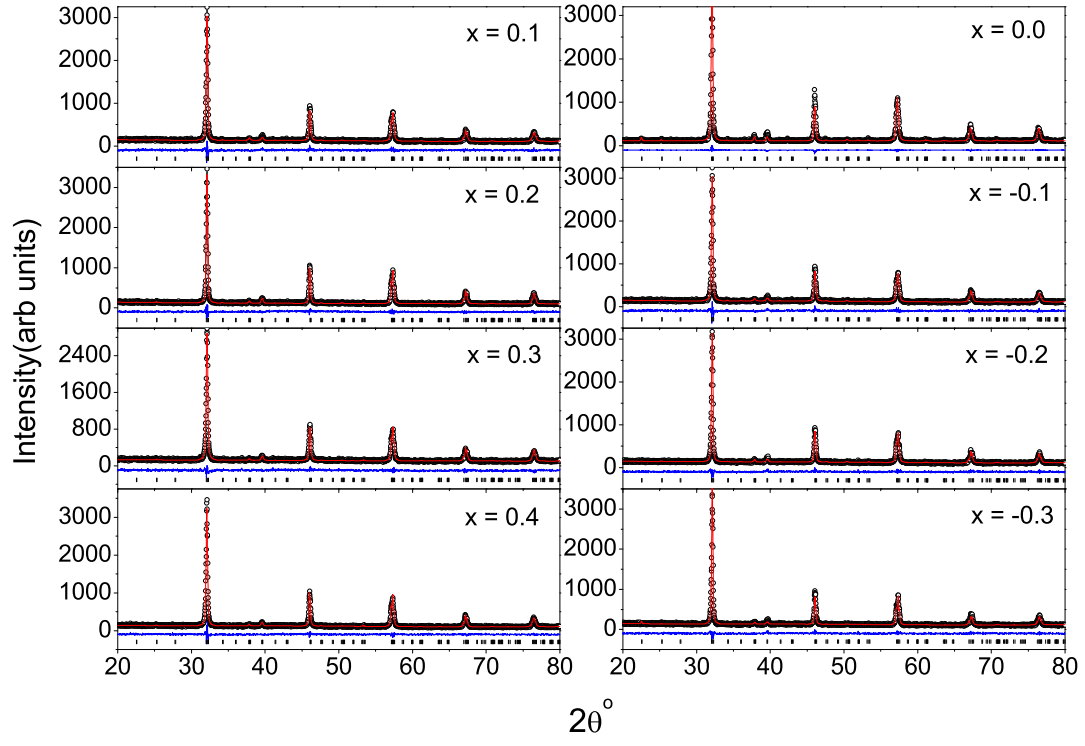


**Fig. 1.** Le bail fitted XRD patterns for  $\text{LaSrCo}_{1-x}\text{Ru}_{1+x}\text{O}_6$ . The data points are indicated as circles and the solid line through them is the fit to the data. The difference pattern is shown at the bottom along with tick marks indicating Bragg reflections.

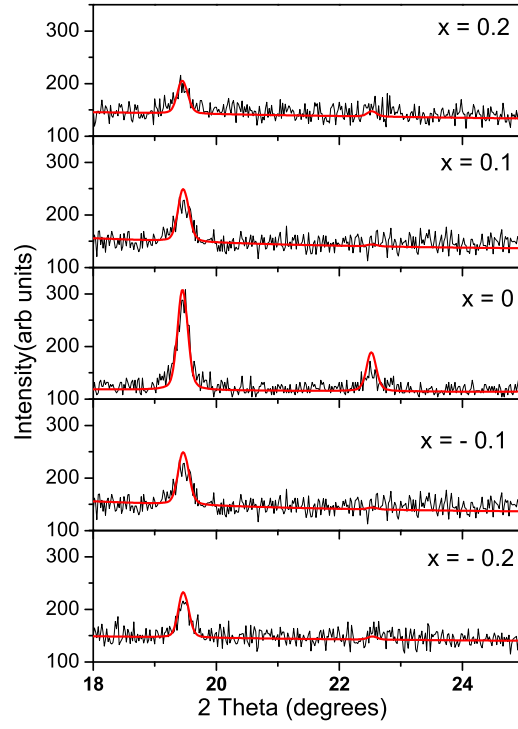


**Fig. 2.** Variation of intensity of superlattice  $(\frac{1}{2}, \frac{1}{2}, \frac{1}{2})$  reflection with increasing Ru ( $x > 0$ ) and Co ( $x < 0$ ) doping.

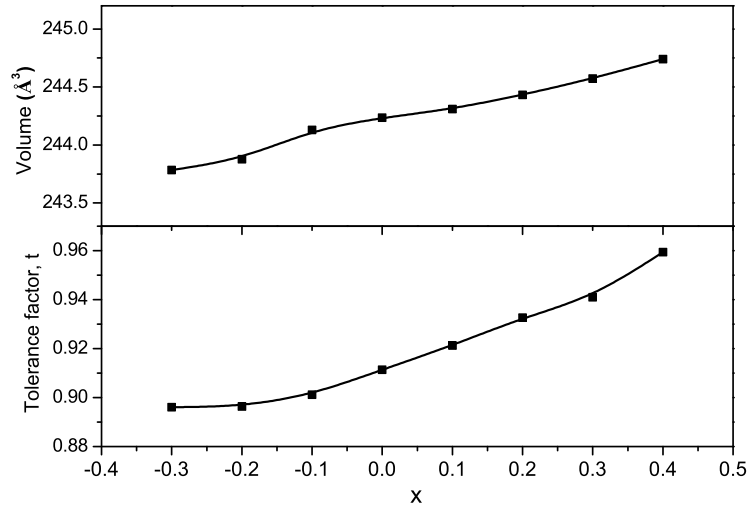


**Fig. 3.** (a) Composition dependence of the unit cell volume in  $\text{LaSrCo}_{1-x}\text{Ru}_{1+x}\text{O}_6$ . (b) Variation of tolerance factor  $t$  with  $x$  in  $\text{LaSrCo}_{1-x}\text{Ru}_{1+x}\text{O}_6$ .



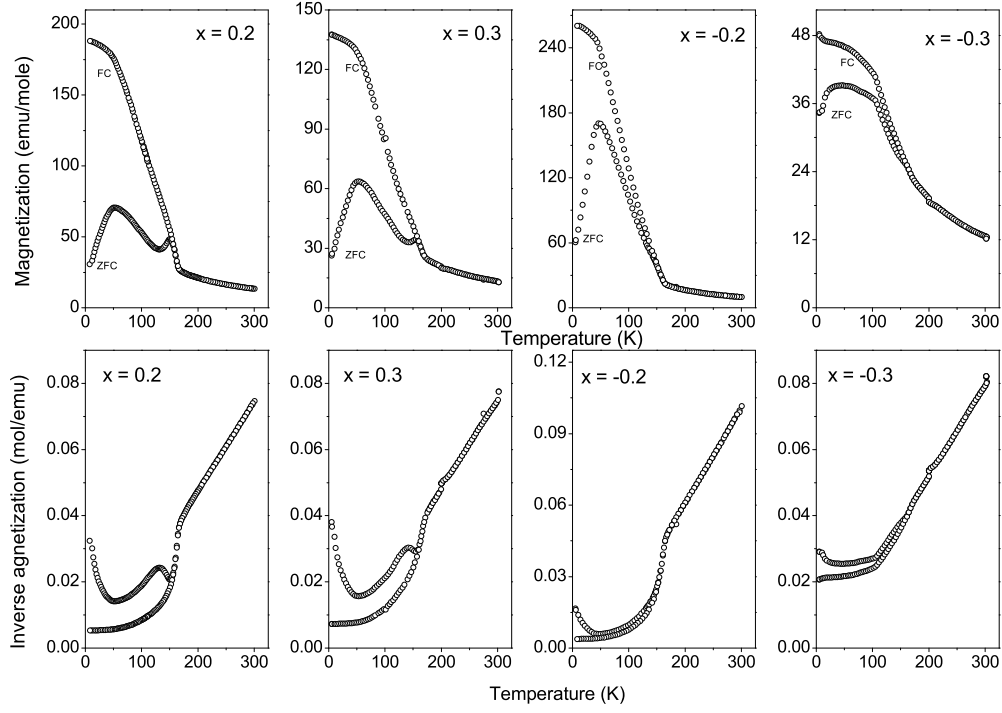


**Fig. 4.** Magnetization curves for  $\text{LaSrCo}_{1-x}\text{Ru}_{1+x}\text{O}_6$  during the ZFC and FC cycle recorded at 1000 Oe.

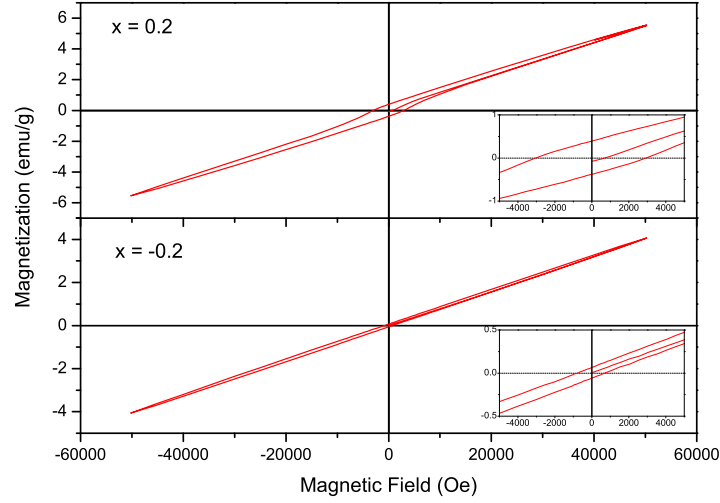


**Fig. 5.** Isothermal magnetization recorded at 5K in the field range of  $\pm 5$ T for two different values of  $x$  belonging to  $\text{LaSrCo}_{1-x}\text{Ru}_{1+x}\text{O}_6$ . Insets show the expanded ( $\pm 4500$  Oe) loops.

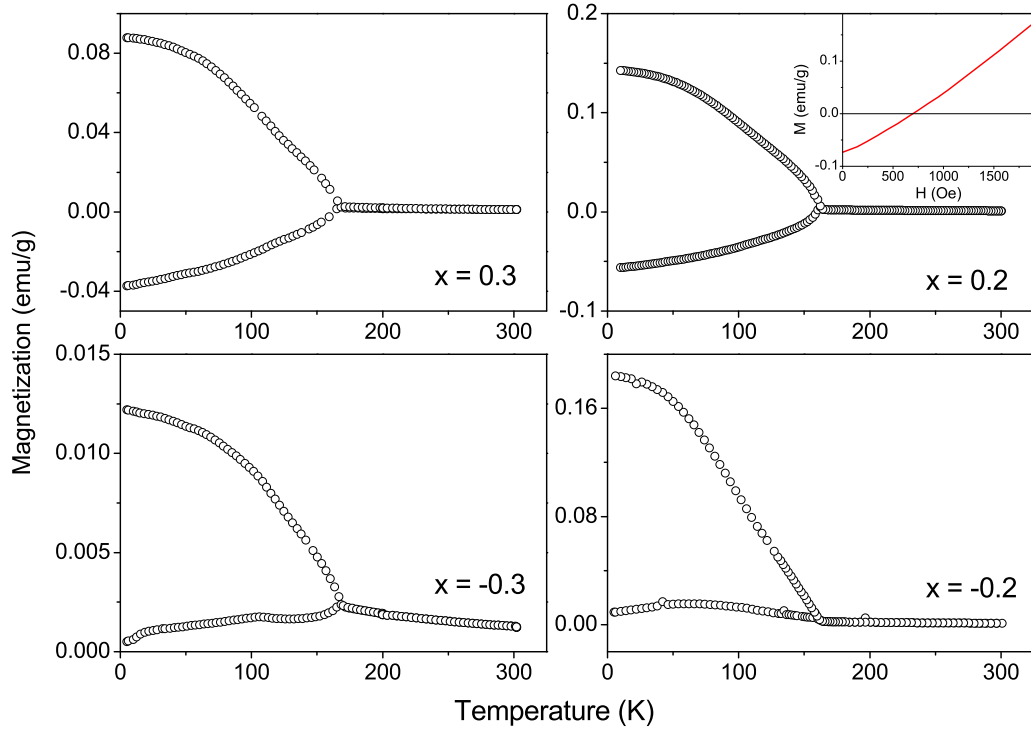


**Fig. 6.** Low field (50 Oe) magnetization data as a function of temperature for  $\text{LaSrCo}_{1-x}\text{Ru}_{1+x}\text{O}_6$ . The inset in plot of  $x = 0.2$  shows the initial magnetization curve as a function of applied field for the same sample.

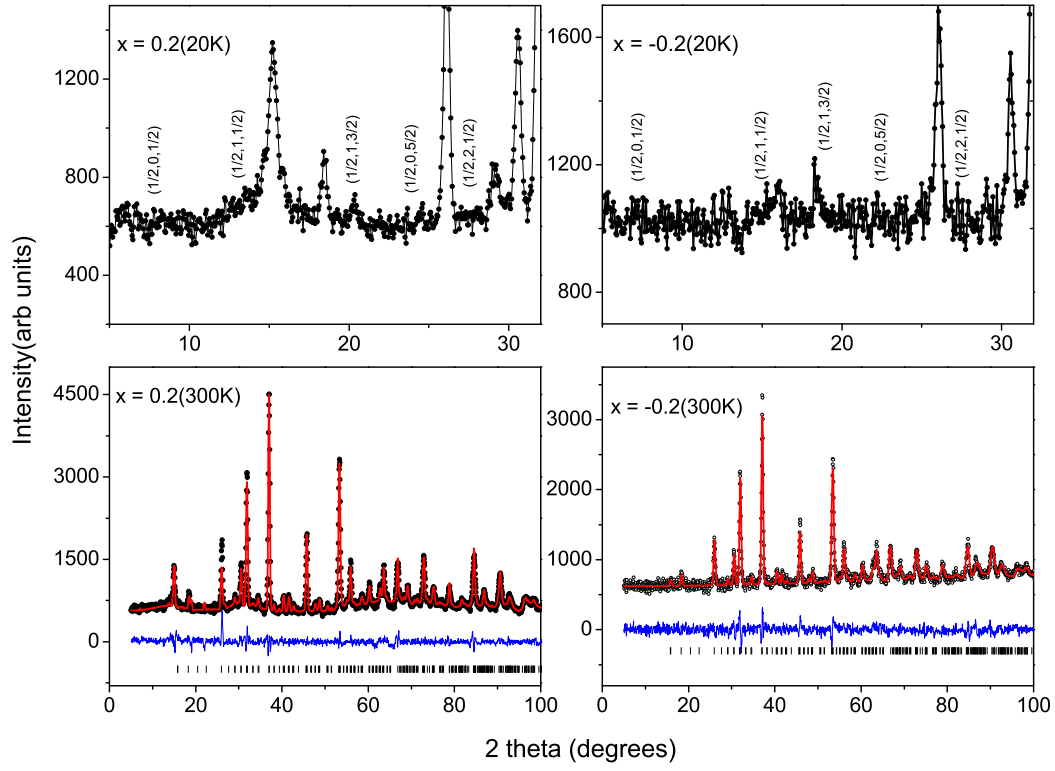


**Fig. 7.** Neutron diffraction patterns recorded at 300K and 20K for  $x = 0.2$  and  $-0.2$  of the series  $\text{LaSrCo}_{1-x}\text{Ru}_{1+x}\text{O}_6$ . The 300K data is presented in the  $2\theta$  range of  $5^\circ$  to  $100^\circ$  as circles along with Rietveld refined curve (solid line through the data) and the difference curve at the bottom. The 20K data is shown in limited range to highlight the weak magnetic reflections (marked with corresponding  $(h,k,l)$  values).

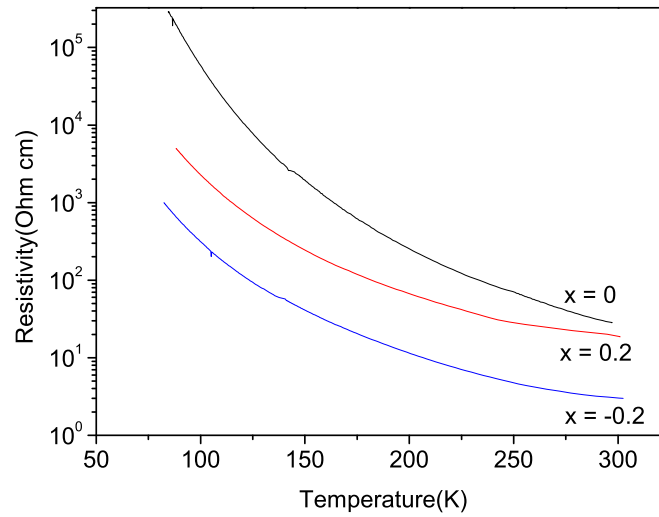


**Fig. 8.** Resistivity as a function of temperature for  $\text{LaSrCo}_{1-x}\text{Ru}_{1+x}\text{O}_6$  compounds where  $x = -0.2, 0$  and  $0.2$

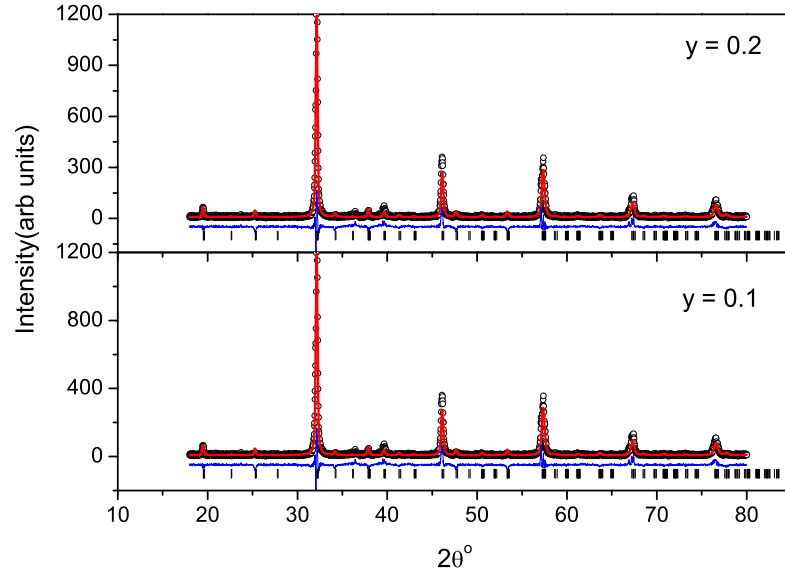


**Fig. 9.** XRD patterns of  $\text{LaSrCo}_{1-y}\text{Cu}_y\text{RuO}_6$  for  $y = 0.1$  and  $0.2$  along with best fitted line and difference line shown at the bottom. The ticks indicate the positions of allowed Bragg reflections.

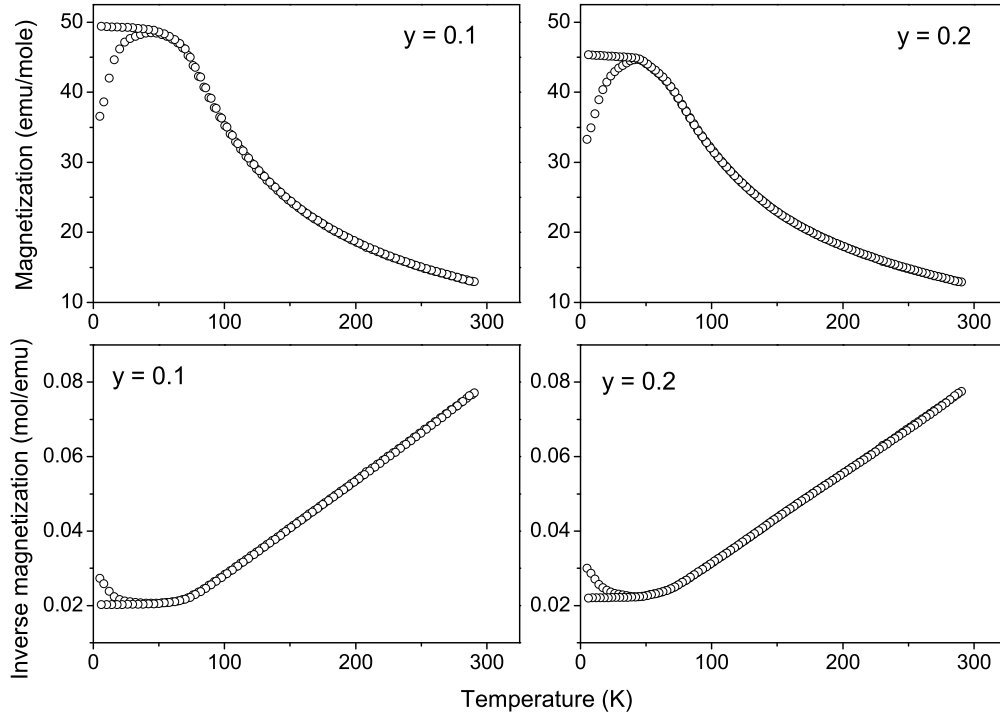


**Fig. 10.** ZFC and FC magnetization curves for  $\text{LaSrCo}_{1-y}\text{Cu}_y\text{RuO}_6$  recorded at  $H = 1000\text{Oe}$ .

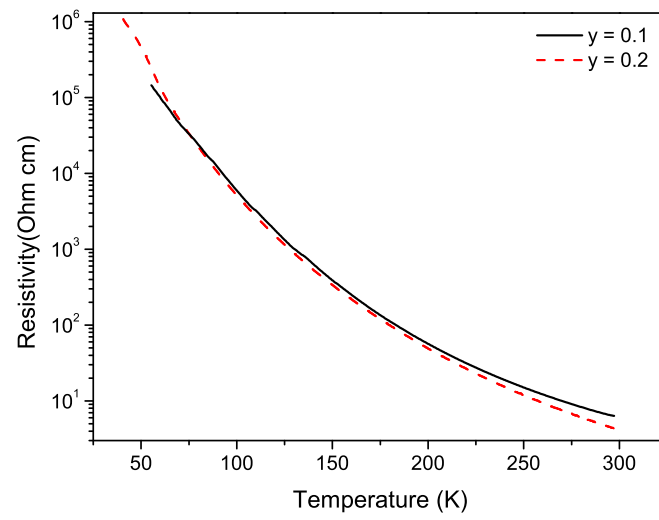


**Fig. 11.** Temperature variation of electrical resistivity for  $\text{LaSrCo}_{1-y}\text{Cu}_y\text{RuO}_6$  where  $y = 0.1$  and  $0.2$ .